Energy 221 (2021) 119901

Contents lists available at ScienceDirect

Energy

journal homepage: www.elsevier.com/locate/energy

Prognostics of battery cycle life in the early-cycle stage based on hybrid model

Yu Zhang [a, b], Zhen Peng [c], Yong Guan [a, b], Lifeng Wu [a, b, *]

[a] College of Information Engineering, Capital Normal University, Beijing, 100048, China
[b] Beijing Key Laboratory of Electronic System Reliability Technology, Capital Normal University, Beijing, 100048, China
[c] Information Management Department, Beijing Institute of Petrochemical Technology, Beijing, 102617, China

ARTICLE INFO

Article history:
Received 24 September 2020
Received in revised form
12 January 2021
Accepted 15 January 2021
Available online 19 January 2021

Keywords:
Lithium-ion battery
Remaining useful life
Early-cycle stage
Random forest
Artificial bee colony
General regression neural network

ABSTRACT

Accurately predicting the remaining useful life (RUL) of lithium-ion batteries in early-cycle stage can speed up the battery improvement and optimization. However, slowly varying and weak predictability of the characteristic quantities in early-cycle stage make it challenging to predict RUL. To overcome this problem, the paper proposes a hybrid prediction model, which integrates random forest (RF), Artificial Bee Colony (ABC) and general regression neural network (GRNN), called RF-ABC-GRNN. First, a new feature space is obtained by performing linear and non-linear transformations on the original features that are slowly changed in early-cycle stage, such as discharge capacity, terminal voltage, discharge current, and internal resistance. Second, RF is used to measure and rank the importance of these new features so as to screen out the high-importance feature combination. Third, the prediction model based on GRNN is constructed. Considering that the smoothing parameter of the model has great influence on the prediction performance, ABC is used for parameter optimization. Finally, in order to verify performance of the model, initial cycles data that have yet to exhibit apparent degradation is used. Comparison results show that the proposed model could effectively screen out the high-importance features and make accurate prediction much earlier.

1. Introduction

Owing to the characteristics of low manufacturing cost, high power density and long useful life, lithium-ion battery has been widely used in portable equipment, electric vehicles and large-scale energy storage systems in recent years [1–4]. However, with the frequency of use increases, the performance of lithium-ion batteries gradually degrades [5–7], which eventually leads to the termination of battery life and causes a series of safety issues [8–11]. Therefore, it is particularly significant to evaluate the safety and reliability of lithium-ion batteries. The health evaluation of lithium-ion batteries includes many aspects, and the RUL prediction is one of the key parts [12–15].

In recent years, with the development of big data and machine learning technology, data-driven lithium-ion batteries health assessment has gradually become a hot spot in the field of battery research, and many related data-driven methods have been proposed [16]. Bian et al. [17] proposed a stacked bidirectional long short-term memory (SBLSTM) neural network is for SOC estimation. Deng et al. [18] proposed a SOC estimation method based on Gaussian process regression (GPR). Li et al. [19] proposed a battery degradation model based on support vector regression (SVR) for capacity estimation. Wu et al. [20] proposed an online RUL estimation method for lithium-ion batteries using a combination of feed forward neural network (FFNN) and importance sampling. Chaoui et al. [21] exploited a recurrent neural network (RNN) method to estimate the charging state and health state of lithium-ion batteries. Yang et al. [22] developed a hybrid neural network method combining long and short term memory (LSTM) neural network and unscented Kalman filter (UKF) for capacity estimation. Ma et al. [23] predicted the RUL by applying a hybrid neural network of extreme learning machine (ELM) and broad learning (BL).

These existing methods have demonstrated promising prediction results, but it is worth noting that these existing studies are all based on long-term historical data during the use of battery. With the improvement of the lithium-ion battery manufacturing

* Corresponding author. College of Information Engineering, Capital Normal University, Beijing, 100048, China.
E-mail address: wulifeng@cnu.edu.cn (L. Wu).

https://doi.org/10.1016/j.energy.2021.119901
0360-5442/

Nomenclatures

ABC	Artificial Bee Colony
ANN	Artificial neural network
BL	Broad learning
CEEMD	Complete ensemble empirical mode decomposition
CNN	Convolution neural network
ELM	Extreme learning machine
FFNN	Feed forward neural network
GRNN	General regression neural network
LSTM	Long and short term memory neural network
MAX_ITER	Maximum iteration
MF	Maximum number of features
MSE	Mean Square Error
NP	Number of populations
NT	Number of decision trees
OOB	Out of pocket data
PSO	Particle swarm optimization
RBF	Radial basis function
RMSE	Root of the mean square error
RF	Random forest
RUL	Remaining useful life
SVR	Support vector regression
SOC	State of Charge
SOH	State of Health
VIM	Variable importance

technology level, the battery cycle life is gradually increasing. Evaluating the life of the battery by taking long-term historical data is not conducive to accelerate the battery development cycle and quickly verify new manufacturing technology. In contrast, accurately predicting the RUL by exploiting the early stage data can accelerate and promote the improvement and optimization of the battery.

In the early stage of battery cycle life, the discharge capacity, terminal voltage, discharge current, internal resistance and other characteristics change slightly, leading to weak RUL prediction ability. These issues make it a challenging task to predict RUL in the early stage. Severson et al. [24] proposed the study of early-cycle stage RUL prediction for the first time. The author built three different feature-based linear model to predict RUL by using only the first 100 cycles data. Among them, the prediction result of the "full" model achieved the lowest average test error of about 9.1% on all testing data sets. However, there are two shortcomings in this approach:

(i) Using a single linear model may not be the best option due to the complexity of internal degradation mechanism, variable parameters and non-linearity of capacity degradation process.
(ii) For the machine learning model, input features have a significant influence on the final prediction result. The combination of features chosen empirically is not necessarily the best. And redundant features are adverse to the prediction performance of model, so it is necessary to compare and select for all features.

Feature selection is a common data preprocessing method [25]. At present, there are mainly two types of feature selection method, namely univariate-based feature selection and model-based feature selection. The main idea of univariate feature selection is to determine the relationship between features variables and response variables by examining each feature individually, such method is easy to realize and understand. But its disadvantage is that redundant features in highly correlated feature subsets can not be eliminated, and this approach ignores the significance of the modeling. Another popular approach is to utilize machine learning models for feature ranking. Many machine learning models have some inherent internal ranking of features or it is easy to generate the ranking from the structure of the model. RF is a popular ensemble model. Its main advantage is that there is almost no need to adjust the parameters manually, and it is not easy to overfit. RF can effectively analyze non-linear, collinearity and interaction data. And it can be able to effectively analyze a small number of samples with high dimension without sacrificing the information in the original feature [26]. RF can give importance metrics for each input feature while analyzing data. Therefore, it is more convenient and effective to use RF as a tool for feature selection [27,28].

As one of the data-driven methods, neural network has strong nonlinear modeling capability, so it is suitable for the degradation assessment of lithium-ion battery. GRNN is a typical artificial neural network (ANN) [29], which has been attracting much attention as its many advantages. Even if the number of samples is small, it can converge to the optimal regression. Compared with traditional ANN, there are fewer parameters that need to be adjusted, and iterative training is not required. Now it has been widely used in the modeling of regression problems [30,31]. However, smoothing parameter is a key parameter in the network, this paper applied the ABC algorithm to determine its value.

Based on the above discussion, this paper proposes a hybrid model called RF-ABC-GRNN for RUL prediction using the early-cycles data, mainly including RF, ABC and GRNN. First, RF algorithm is used to calculate the importance of each feature in the feature space for ranking. The combination of features with higher importance is selected as the input of the prediction model to avoid excessive prediction error caused by too many useless features and reduce the complexity of the model. Second, ABC algorithm is used to determine the smoothing parameter value in GRNN to further improve the prediction performance. Finally, experiments are carried out to verify the proposed algorithm. Comparison results show that the proposed model could effectively screen out the high-importance features and make accurate prediction much earlier.

2. Methods

2.1. Random forest

RF is an intelligent ensemble learning algorithm [26] based on decision tree, which consists of bagging method and random node optimization. A series of decision trees are generated and combined to obtain more accurate and stable forecasts. Its structure is shown in Fig. 1.

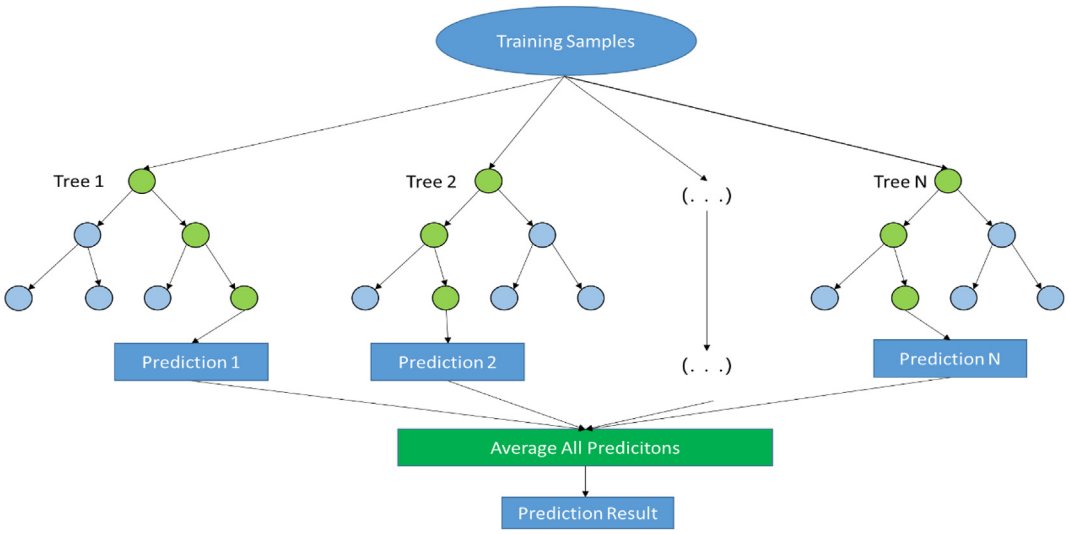

Fig. 1. Flow chart of random forest.

The algorithmic process of RF is given in Algorithm 1.

Algorithm 1: Random forest
Input: 1) data set *D*, 2) number of decision tree *NT*, 3) max features *MF*.
Output: Predictions combined by averaging the results of each decision tree.
1. **for** $i = 1$ to *NT*
2. Draw a bootstrap sample $D_t$from *D* with replacement to generate training sets for each decision tree.
3. Use each training set to build a decision tree, and the process of generating a decision tree does not require pruning processing.
4. **end for**
5. **return** the average results

The data not extracted during training process is called out of pocket data (OOB). Since OOB data is unbiased, the mean square error value of OOB data can be used to evaluate the degree of influence of independent variables on dependent variables, namely variable importance (VIM).

The specific steps of the calculation process are as follows:

VIM calculation process

Step1: Use the corresponding OOB (out-of-bag data) data of each decision tree in RF to calculate its out-of-bag data error MSE_{oob}.
Step2: Randomly replace the target feature variable X_i , and calculate its out-of-bag data error MSE_{oobi} again.
Step3: Use the number of decision trees to divide the difference between MSE_{oob} and MSE_{oobi} to get the average.
Step4: Use standard deviation standardization (z-score standardization) to obtain the VIM value of the feature variable X_i.

2.2. Artificial Bee Colony

ABC is a swarm intelligence optimization algorithm [32], which including three types of artificial bees: employed bees, onlooker bees, and scout bees. The position of the food source represents the feasible solution, and the quality of the food source represents the fitness value of the feasible solution. The best food source is found by simulating the behavior of food source searching and greedy selection mechanism of nearest neighbor search.

Let x_i denote the location of current food source, the new food source is obtained by

$$N(k+1) = x_i(k) + \phi(x_i(k) + x_t(k)) \tag{1}$$

where x_t is a randomly selected food source, k represents the iteration number. The fitness value between new food sources and existing food sources is compared to retain the better food sources until the end of the iterations. And the onlooker bee chooses the food source by

$$p_k = \frac{fit(x_i(k))}{\sum_k^{NP} fit(x_i(k))} \tag{2}$$

The pseudocode is given in Algorithm 2.

Algorithm 2: Artificial Bee Colony Algorithm
Input:1) number of population NP, 2) limitation range *limit*, 3) max number of iterations MAX_ITER, 4) number of food source SN
Output: the optimal solution
1. Generate the initial population
2. **for** k = 1 to MAX_ITER
/*Employed Bee Stage*/
  for i to SN
    find the new food source near the current food source according to Equation (1)
  end for
/*Onlooker Bee Stage*/
  for i to SN
    send onlooker bees to food source according to Equation (2)
    find the new food source near the current food source according to Equation (1)
    evaluate the fitness value and apply greedy selection to retain the better solution
  end for
/*Scout Bee Stage*/
  if *limit* is reached
    send the scout bee to a randomly selected food source
  end if
  record the best solution so far
end for
return the best solution

2.3. General regression neural network

GRNN is a modified form of radial basis function (RBF), which has strong nonlinear approximation ability, high fault tolerance. It is suitable for small samples issues. Only the smoothing parameter parameters need to be determined during the calculation process. The structure of GRNN is shown in Fig. 2, which consists of four layers: input layer, pattern layer, summation layer and output layer. The corresponding input sample X is defined as $X = [x_1, x_2, x_3, \ldots, x_n]^T$, and the output sample Y is defined as $Y = [y_1, y_2, y_3, \ldots, y_m]^T$.

(1) Input layer

The input layer is used to receive the input samples, and the number of neurons is equal to the feature dimension of the samples.

(2) Pattern layer

The number of neurons in the pattern layer is depends on the number of samples n, each neuron corresponds to different samples. The transfer function of neurons in the pattern layer is defined as following equation:

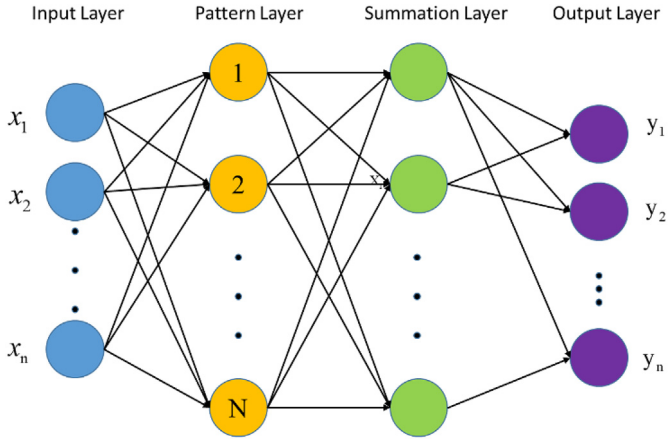

Fig. 2. Architecture of GRNN.

$$p_i = \exp\left(-\frac{(X - X_i)^T (X - X_i)}{2\sigma^2}\right), (i = 1, 2, 3, \ldots, n) \quad (3)$$

where$X$represents the input variable of the network, $X_i$represents the corresponding sample of the i^{th} neuron.

(3) Summation layer

There are two kinds of neurons for summation in the summation layer. One layer sums up all output results of GRNN neural network, the connection weight between the independent neuron and the pattern layer is 1, and the transfer function is:

$$S_D = \sum_{i=1}^{n} p_i \quad (4)$$

The other one layer calculates the weighted sum of output of the neurons of the pattern layer, and the transfer function is given as:

$$S_{Nj} = \sum_{i=1}^{n} y_{ij} p_i, (j = 1, 2, 3, \ldots, m) \quad (5)$$

where y_{ij} represents the weight between the neurons in the pattern layer and the neurons of the summation layer. And it is the jth element in the ith output sample.

(4) Output layer

The dimension of the final training output vector of the neural network depends on the number of neurons, and the result of the sum layer above is divided by the neurons to obtain the final result:

$$y_j = \frac{S_{Nj}}{S_D}, (j = 1, 2, 3, \ldots, m) \quad (6)$$

where yj represents the output of the jth node in the output layer.

2.4. Early-cycle stage RUL prediction framework based on RF-ABC-RFR

The overall framework of the RF-ABC-RFR model constructed in this paper is shown in Fig. 3. The model is mainly divided into three

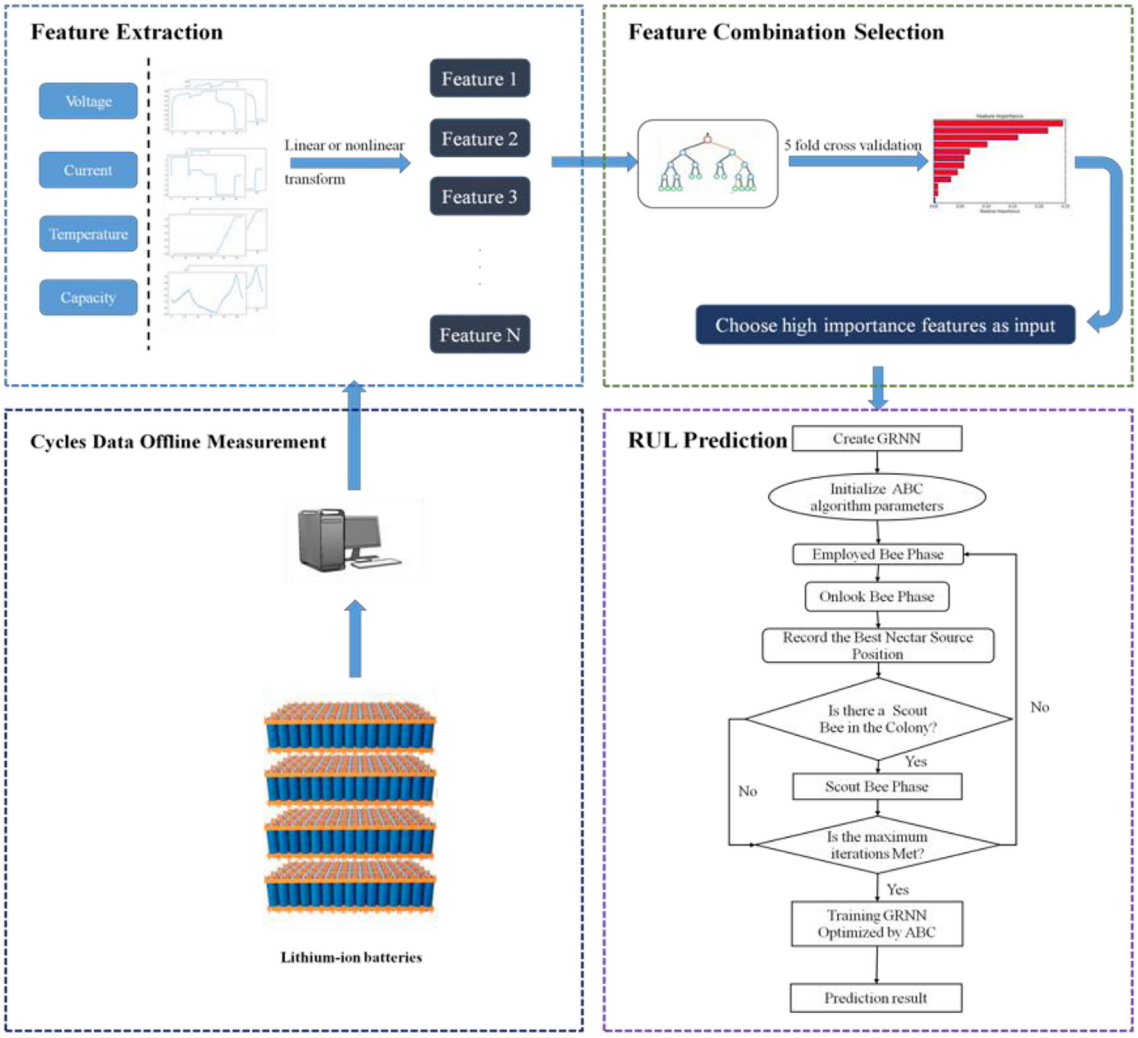

Fig. 3. RUL prediction framework diagram based on the RF-ABC-GRNN model in the early-cycle stage.

parts.

The first part is feature extraction. First, according to the off-line measured cycling data, the characteristic data of capacity, voltage, current and internal resistance recorded in the early cycle of the battery are extracted. Then the enhanced new features are obtained by performing linear and nonlinear transformation on these original features.

The second part is feature combination selection. First, RF model is established. All the samples constructed by new features are input into the model for training. The real RUL values are taken as the output of the model. Second, the model is trained by 5-fold cross validation, and the results of feature importance returned by the model are calculated and sorted. Finally, the features with high importance are retained as the input of the prediction model.

The third part is the RUL prediction. According to the features selected in the second part, the number of input neurons of GRNN is determined. Then the GRNN is established. Next, the ABC algorithm parameters are initialized, and smoothing parameter of GRNN is used as a food source to find its optimal solution through repeated iterations. Finally, the parameters are substituted into GRNN to obtain the final RUL prediction result.

3. Description of experimental data

3.1. Data set introduction

In this study, two different data sets are used for experimental investigation, the first data set used in this study is provided by Ref. [24](referred to as NE in this paper), which consists of 124 commercial LFP/graphite batteries (A123, APR18650M1A, rated capacity 1.1Ah, nominal voltage 3.3V), and it is divided into three batches according to the test date. All the batteries are tested in a constant temperature chamber of 30 °C, using 72 different charge strategy but same discharge strategy (from 4C to 2.0V, where 1C represents 1.1A) on a 48-channel Arbin LBT potentiostat. The test obtained totaling 96,700 cycles information, where the cycle lives range from 150 to 2300. The data set mainly contains the continuously measured voltage, current, and temperature of each battery during every cycles. In addition, it also contains the charge and discharge capacity value of each cycle, the number of cycle life of each battery, and other data that can be derived from the above. According to the author, this data set is currently the largest published commercial battery cycle data set.

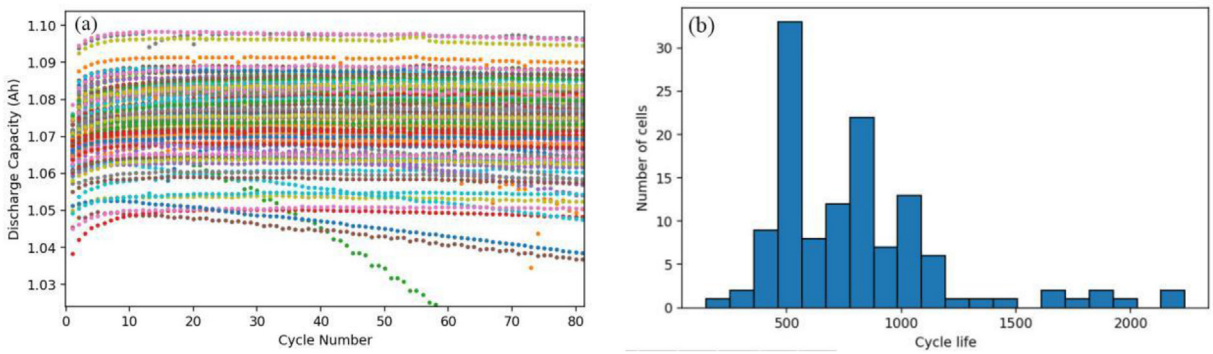

Fig. 4. Data depiction. (a) The relationship between the discharge capacity of the first 80 cycles and the number of cycles and (b) Histogram of battery life distribution.

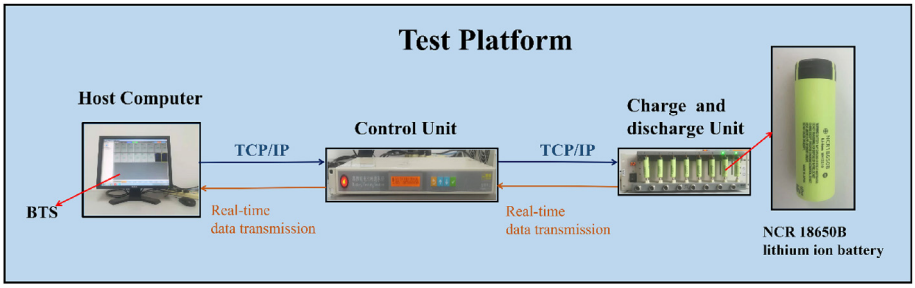

Fig. 5. Test platform.

Some basic descriptions of this data set are shown in Fig. 4. And Fig. 4(a) is the capacity degradation curve of the first 80 cycles. It can be seen from the figure that the capacity degradation of the first 80 cycles is weak, and there is no obvious decline. Fig. 4(b) shows the life distribution of these 124 batteries, where most of the battery life is more than 500 times.

In addition to recording the raw data during the battery cycle, the author also contributes 20-dimension features extracted from these raw data.

The second data set used for investigation is obtained from our own test platform (referred to as OB in this paper). Fig. 5 shows the experimental setup of this platform. The test platform consists of three main parts, host computer with a battery test system (BTS), control unit, and charge and discharge unit. The host computer sends commands to the control unit to connect with the charge-discharge unit through TCP/IP port. The charge-discharge is responsible for controlling the charge/discharge channel and collecting the voltage, capacity and other data in real time.

Five NCR18650b $LiNiCoAlO_2$ batteries produced by the same manufacturer are used for cycle test. The key specifications of the tested battery are given in Table 1. The five batteries are charged with constant current and constant voltage strategy. Then they were divided into two groups according to different discharge strategies. The first group includes B1, B2 and B3. Variable current discharge strategy is adopted for these batteries. The second group includes B4 and B5, and constant current discharge strategy is adopted for the two. After a series of cycle tests, the degradation data of five batteries are obtained, and the capacity degradation curves are shown in Fig. 6. The cycle life of these batteries is around 160 times. It can be observed from the local enlarged view that the capacity degradation of all batteries is weak in the early stage of cycle life (about the first 25 cycles), and the degradation rate begins to accelerate with the cycle number increasing.

Table 1
Description of the tested battery.

Parameters	Value
Capacity	3.4Ah
Min/Max voltage	2.75V/4.25V
Rated voltage	3.7V
Min/Max temperature	−20 °C/60 °C

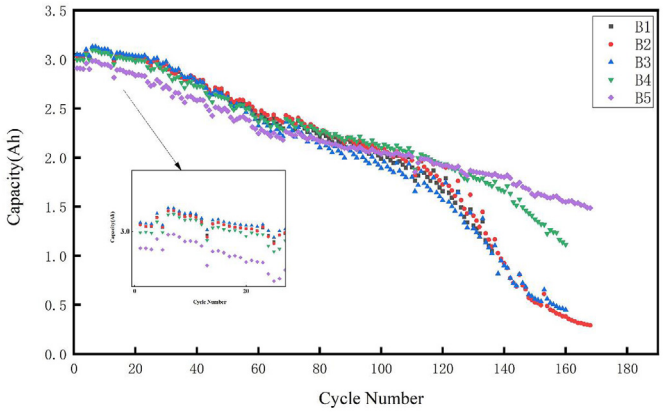

Fig. 6. Capacity degradation curves of the five batteries.

3.2. Data set division

In order to compare with the results in Ref. [24], the division of the NE data set is same as [24]. The 124 batteries in the NE data set are divided into three parts, training set, testing set and secondary testing set. Among them, 41 batteries in the training set are used to train the model, and 43 batteries in the testing set are used to test

the model performance. The remaining 40 batteries in the secondary testing set are used to evaluate the robustness of the model.

Considering the limited sample size, the leave-one-out cross validation is used for the OB data set. When one of the batteries is used for testing, the others are used for model training. For example, B1 is used for testing, while B2, B3, B4, B5 are used for training, the rest can be done in the same manner.

4. Experimental comparison

The overall goal of this paper is to show that the proposed method can accurately predict the RUL of lithium-ion batteries in the early-cycle stage. More specifically, it is to show that the proposed method can predict RUL earlier and more accurately under the same data constraints.

4.1. Feature selection based on RF

Each feature in the feature space has a certain influence on RUL, but their influence degrees are different. Instead of improving the prediction accuracy, the features with low influence increase the computation complexity. Therefore, it is necessary to screen out the high-importance features before performing RUL prediction.

Basically, the aim of feature selection is to model the target variable with a subset of important input variables. High-dimensionality of the features makes the visualization and interpretation difficult. As a predictor, RF performs an implicit feature selection by using only a small number of "strong feature" for prediction, and thus performs well in high-dimensional data. The results of implicit feature selection can be visualized by using VIM measures, which can reflect the contribution of each feature to the prediction result and measure the corresponding prediction ability. However, prediction accuracy is not the only criterion for measuring a predictor, but also efficiency. Therefore, the best feature combination of the two indicators is served as a basis for distinguishing the best feature combination.

Take the first 100 cycles as an example. First, RF is used to calculate the VIM of all features by the steps described in Section 2.1, the calculation results are sorted and numbered from 1 to 20 as shown in Fig. 7. And the feature names and corresponding abbreviations is given in Supplementary Table 1. Second, according to the ranking order, the feature dimension is continuously increased to the predictor to calculate the prediction accuracy (as shown in Fig. 8) and the time consumption (as shown in Fig. 9). Third, the feature dimensions were scored from 1 to 20 according to their prediction accuracy and time consumption separately. The higher the prediction accuracy, the higher the score. On the contrary, the more time consumption, the lower the score. Finally, the total score of the feature combinations is calculated. The feature combination with a total score less than 20 is considered as a low-importance combination, while the feature combination with the scores ranked in the top 1/3 is considered as a high-importance combination. After calculation, features with the importance higher than 0.30 are called high-importance features, which have a significant impact on the final result, and those with importance between 0.15 and 0.30 are called medium importance features, while those less than 0.15 are called low-importance features, indicating their effects are negligible. Based on the above analysis, four features are selected: variance, skewness, the fitting slope of the 2nd to 100th cycle discharge capacity curve, and the internal resistance difference between 100th and 2nd.

4.2. Evaluation function

In order to evaluate the accuracy of RUL prediction of the proposed method and make a fair comparison with existing work, two functions used in Ref. [24] are selected as evaluation function in this paper. These two functions are specifically defined as follows:

$$RMSE = \sqrt{\frac{1}{m}\sum_{i=1}^{m}\left(y_i - \hat{y}_i\right)^2} \tag{7}$$

$$\%\text{err} = \frac{1}{m}\sum_{i=1}^{m}\frac{|y_i - \hat{y}_i|}{y_i} \times 100 \tag{8}$$

where y_i represents the real RUL, $\hat{y}_i$ represents the predicted RUL, m is the total number of samples.

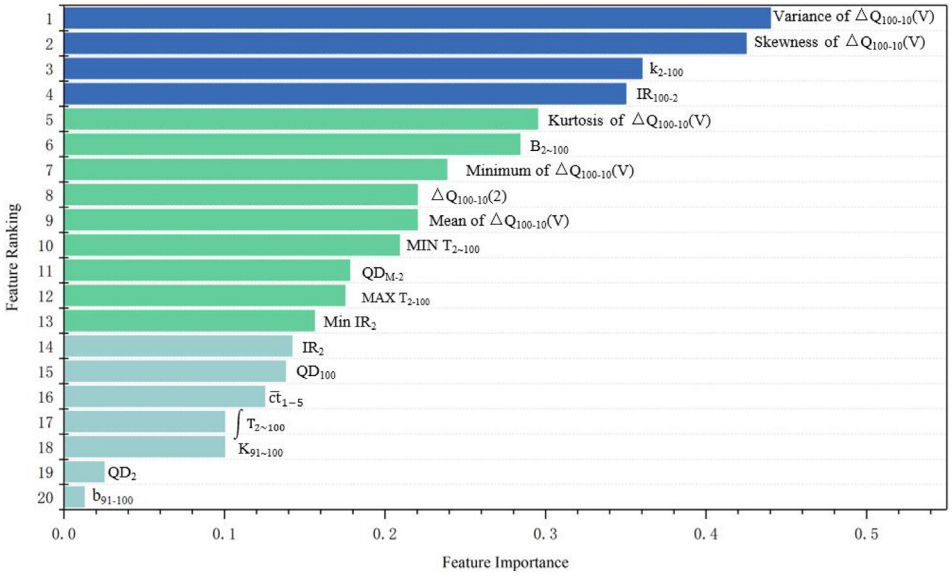

Fig. 7. Importance ranking of all features.

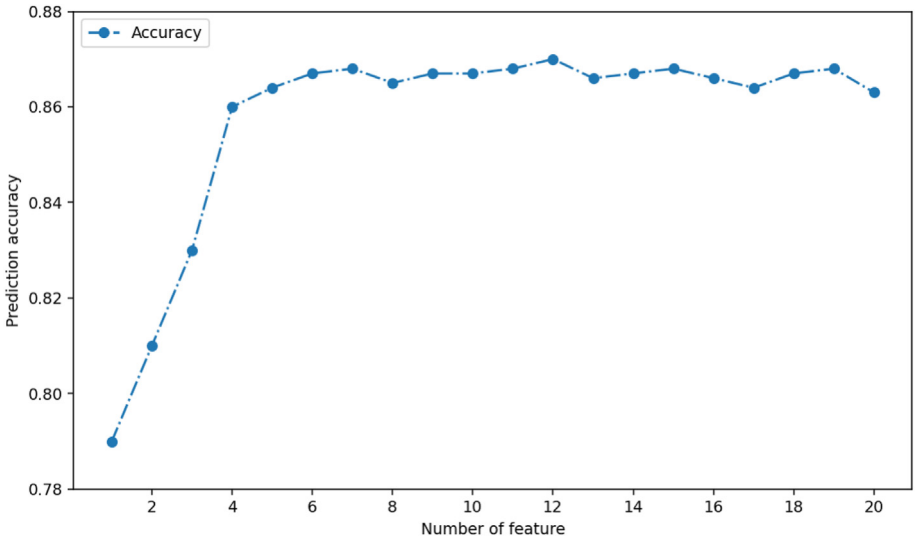

Fig. 8. Relationship between the prediction accuracy and feature number.

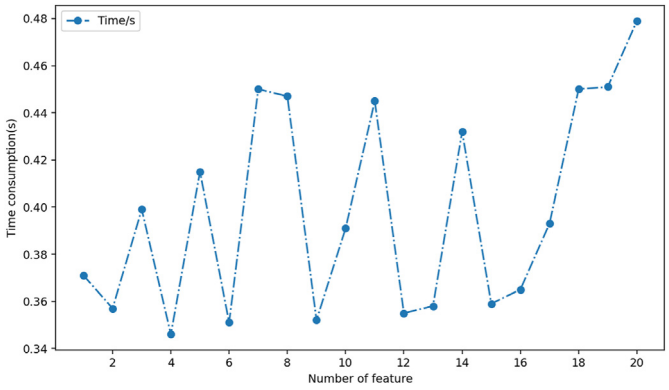

Fig. 9. Relationship between time consumption and feature number.

4.3. Experiment results analysis

In order to evaluate the effectiveness and accuracy of the proposed method, two cases of experiment are performed on the NE data set and OB data set, respectively.

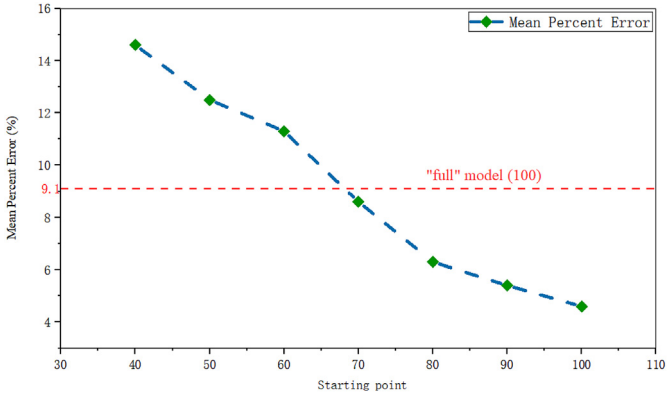

Fig. 10. The test error under different quantitative cycle data.

4.3.1. Case 1: NE data set

The experiment of Case 1 is mainly divided into two parts: one is to quantitatively use the data before a certain cycle number in the early stage, and the other is to use the early-stage data of cycle life according to a certain proportion.

In literature [24], the author established three linear models with different input based on the features extracted from the first 100 cycles (the input feature combinations of the three models are detailed in Ref. [24]). Among them, the "full" model achieved the best prediction accuracy for about 9.1% test error. This paper applied it as a baseline to evaluate the performance of the proposed method.

One of the goals of this paper is to investigate whether the proposed method could accurately predict the RUL earlier. Seven different quantitative early cycles are selected for this investigation, including the first 40, 50, 60, 70, 80, 90, 100 cycles. The prediction results of the seven cases are shown as Fig. 10.

As shown in Fig. 10, the green point represents the prediction results under different cases, and the red reference line represents the given result in Ref. [22]. It can be seen from the Fig. 10 that the proposed approach is superior to the baseline in using the first 100 cycles. In the case of some lower cycle numbers, the proposed method can also be superior to this result, such as 70, 80 and 90 cycles, which reflects the superiority of the proposed method again. Additionally, it is common knowledge that data-driven methods can perform better with more training data. Conversely, less data can lead to performance degradation, and all the results have revealed this trend. For the first 60 cycles and earlier cases, the model obtained the worse results than the baseline, indicating that the performance of the model has reached the upper limit due to the limitation of data scale.

In order to further demonstrate the performance of the model, the prediction results based on the first 80 cycles are selected to compare with the baseline result for further analysis. Fig. 11 shows the prediction results comparison on two testing set, where the blue columns represent the real RUL of the battery, the blue scatters represent the prediction result of the "full" model, and the red scatters represent the prediction result of RF-ABC-GRNN. It can be seen from Fig. 11 that the overall prediction results of proposed model are closer to the real RUL value than those of the "full" model. Especially for the batteries with long life, the prediction results of the proposed method are greatly improved compared to

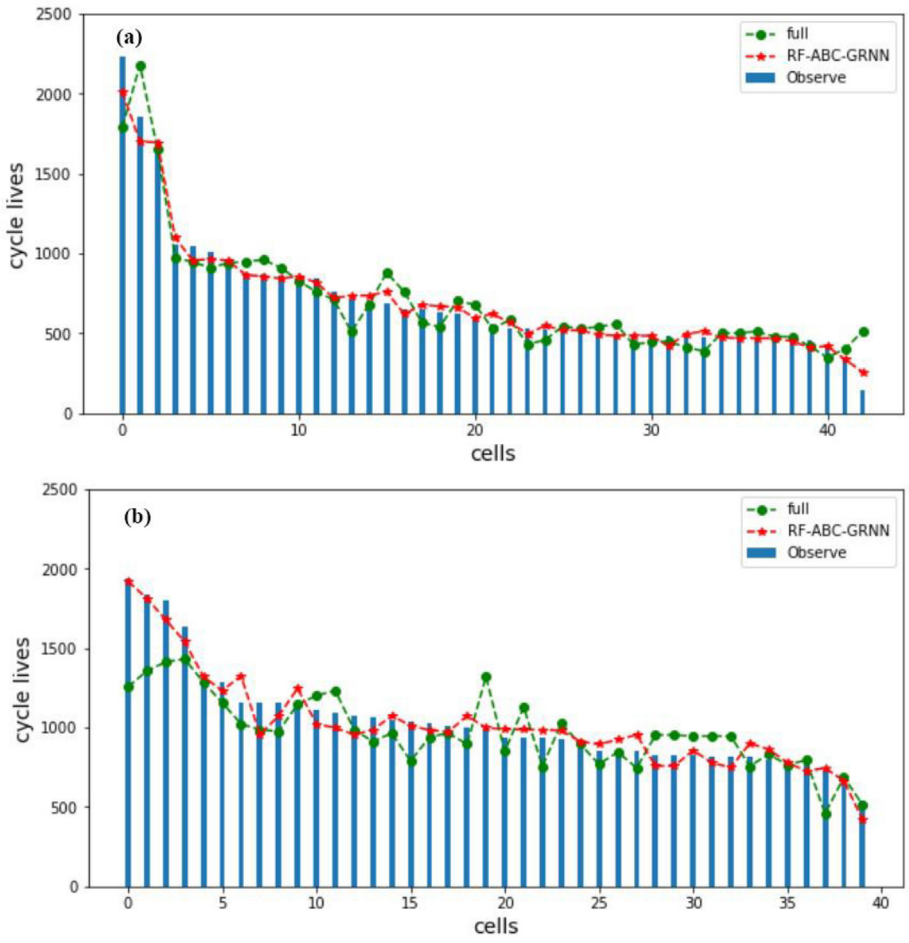

Fig. 11. Prediction results comparison on two testing set. (a) The prediction results on the testing set. (b) The prediction results on the secondary testing set.

Table 2
Prediction results comparison of the eight algorithms. Severson et al. consider that the battery with the shortest life span is an outliner. Therefore, the prediction results after excluding this battery are shown in parentheses.

Algorithm	Starting points	RMSE (cycles)			Mean percent error (%)		
		Train	Primary test	Secondary test	Train	Primary test	Secondary test
"full" (baseline)	100	51	118 (100)	214	5.6	14.1 (7.5)	10.7
FFNN	80	56	130 (126)	230	7.0	15.5 (9.2)	11.4
SVR	80	58	138 (131)	256	6.8	15.8 (8.9)	12.7
GRNN	80	52	120 (93)	218	6.5	14.2 (7.8)	12.4
ABC-SVR	80	54	112 (93)	205	5.4	12.8 (6.7)	9.7
PSO-GRNN	80	51	125 (89)	232	5.8	14.3 (8.8)	11.9
ABC-GRNN	80	45	115 (82)	202	4.5	13.0 (6.4)	9.6
RF-ABC-GRNN	80	39	80 (76)	174	2.1	9.8 (5.1)	7.5

the "full" model, which shows that RF-ABC-GRNN has better modeling capability for long-term nonlinear degradation processes than linear model.

In addition to the existing work, feed forward neural network (FFNN) [20], support vector regression (SVR) [33], GRNN [34], ABC-SVR [35], PSO-GRNN [36] and other algorithms are also introduced for comparison. The same training method is used to train these algorithms, and the prediction results of the "full" model is cited from Ref. [24] as a baseline. In order to ensure a fair comparison, the input feature combination of the "full" model is used as the input of these model. Finally, the evaluation function in Section 4.2 is used to calculate the prediction results of all models. The results are shown in Table 2.

Table 2 demonstrates that the proposed method is superior to other methods in all cases in using the first 80 cycle data. And the proposed method reaches a lower test error of 6.3% than 9.1% of the baseline. These results further illustrate the effectiveness of feature selection. The prediction accuracy of RF-ABC-GRNN with feature selection is 3.2% higher than that of ABC-GRNN using "full" model features as input, which shows that the selected features can effectively improve prediction accuracy. At the same time, through feature selection, the complexity of ABC-GRNN model is reduced, which also contributes to the improvement the performance of the model.

In addition, in order to investigate the RUL prediction performance of several models on the batteries with large life differences

Table 3
RUL prediction results of eight models for two batteries with different cycle life.

Algorithm	Starting point	EL150800460623				EL150800460673			
		R_t	R_p	E_{RUL}	PE_{RUL}	R_t	R_p	E_{RUL}	PE_{RUL}
"full" (baseline)	80	2157	1689	548	24.5%	255	289	34	13.3%
FFNN	80	2157	1654	583	26.1%	255	295	40	15.7%
SVR	80	2157	2756	519	23.2%	255	219	36	14.1%
GRNN	80	2157	1712	525	23.5%	255	221	34	13.3%
ABC-SVR	80	2157	2689	452	20.2%	255	278	23	9.0%
PSO-GRNN	80	2157	2712	475	21.2%	255	281	26	10.2%
ABC-GRNN	80	2157	1859	378	16.9%	255	235	20	7.8%
RF-ABC-GRNN	80	2157	1945	292	13.1%	255	269	14	5.5%

under the same data constraints, two batteries with different life in the testing set (battery 1 EL150800460514 has a cycle life of 2237 times, Battery 2 EL150800460673 has a cycle life of 335 times) are selected for analyses separately. The linear model is used as a baseline model for comparison again. The error between the prediction result and the true RUL is defined as:

$$E_{RUL} = |R_t - R_p| \tag{9}$$

$$PE_{RUL} = \frac{|R_t - R_p|}{R_t} \times 100\% \tag{10}$$

where R_t represents the real RUL value, R_p represents the predicted RUL value. The smaller the value of $PE_{RUL}$and E_{RUL}, the higher the prediction accuracy of the model.

The prediction results of the eight algorithms on these two batteries are shown in Table 3.

From the results in Table 3, it can be concluded that under the same early data constraints, the prediction accuracy of RF-ABC-GRNN is higher than that of other models. Especially for the No.1 battery with long life, the prediction results of RF-ABC-GRNN are much better than other models, which indicating that the proposed model has stronger modeling ability and better prediction performance for long-term nonlinear process. Overall, in terms of quantitatively using early-cycle data for RUL prediction, RF-ABC-GRNN can predict the RUL earlier and more accurately than existing work and other methods.

The prediction result comparison in the case of using the several different quantitative cycles data is introduced. However, considering the discrete distribution of battery life and the large span (the life range is 150–2300 times), a certain number of cycles is not the same early stage for batteries with different life span. Therefore, this paper decided to take the same proportion of the early-cycle data from the data set to train these models to further analyze their prediction ability.

First of all, the data set division mentioned in Section 3.2 is still used. Then the first 10% and the first 30% of all battery cycle life data in the training set are taken as two groups of training data. All models are trained by the same training method as in previous section.

Finally, the prediction results of all models are shown in Table 4.

From Table 4, it can be seen that the prediction errors of RF-ABC-GRNN are also smaller than other models in the two cases. It should be noted that compared with ABC-GRNN that using the "full" model features as input, the mean percent error of RF-ABC-GRNN decreased from 13.05% to 9.35%, 9.9%–6.65% in using the first 10%, 30% cycles respectively. This result verifies the importance of feature selection again. Additionally, the prediction results of the eight models using the first 30% cycles data are better than the prediction results using the first 10% cycles data, which also shows that the proportion of degradation data selection also exerts a significant impact on the experimental results.

Overall, RF-ABC-GRNN can accurately predict the RUL of lithium-ion batteries in the early-cycle stage than other methods in using the same proportion of early-cycle data for RUL prediction.

4.3.2. Case 2: OB data set

In this case, the OB data set is used to further explore the generalization performance of the proposed method. The same parameter setting and training strategy as in the previous case are used again.

Considering that the degradation of the batteries before the first

Table 4
RUL prediction results of eight models using the first 10% and the first 30% cycle data.

Algorithm	Proportion	RMSE (cycles)			Mean percent error (%)		
		Train	Primary test	Secondary test	Train	Primary test	Secondary test
"full" (baseline)	10%	78	132 (125)	240	9.9	17.4 (11.5)	14.6
	30%	45	98 (84)	196	7.5	14.5 (8.6)	11.2
FFNN	10%	74	140 (135)	230	10.4	18.5 (12.8)	14.1
	30%	58	110 (95)	201	8.2	15.6 (9.1)	12.5
SVR	10%	85	125 (116)	235	11.4	17.5 (10.9)	15.7
	30%	51	111 (92)	188	7.6	16.2 (8.5)	12.7
GRNN	10%	96	124 (110)	224	12.4	16.8 (11.4)	12.4
	30%	43	98 (85)	179	8.5	14.2 (7.7)	11.4
ABC-SVR	10%	70	111 (99)	212	10.1	16.2 (10.4)	13.0
	30%	38	87 (77)	165	7.7	14.8 (9.9)	10.7
PSO-GRNN	10%	74	120 (112)	205	9.5	14.5 (10.0)	13.4
	30%	30	78 (67)	158	7.2	13.4 (8.5)	11.1
ABC-GRNN	10%	51	107 (95)	198	8.4	13.5 (9.5)	12.7
	30%	28	75 (61)	147	6.8	10.4 (6.4)	9.6
RF-ABC-GRNN	10%	40	85 (75)	185	6.9	11.2 (8.0)	10.7
	30%	21	68 (55)	132	4.6	9.7 (5.1)	8.2

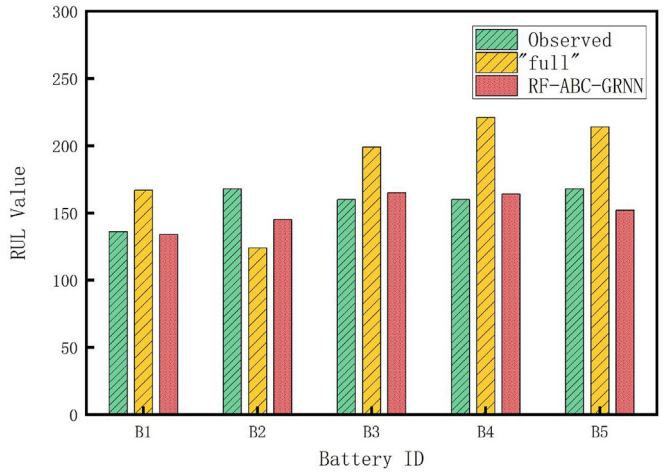

Fig. 12. Histogram of comparison results.

25 cycles is weak, the first 25 cycle data is used for prediction in this case. The final prediction results are shown in Fig. 12, and the baseline model is introduced as comparison.

As shown in Fig. 12, the green columns, orange columns and red columns represent the real RUL value, the prediction result of "full" model and the prediction result of RF-ABC-GRNN, respectively. It can be directly seen form this figure that the prediction results of the proposed method are much closer to real value on all tested batteries. This result verifies the effectiveness and superiority of the proposed method again. And it shows that the proposed method has good robustness.

5. Conclusions

In order to accurately predict the RUL of lithium-ion battery in the early stage of battery cycle life, this paper proposes a hybrid model called RF-ABC-GRNN, which integrates RF, ABC and GRNN. RF is used to screen out the feature combination with high importance as the input of prediction model. ABC algorithm is used to optimize the smoothing parameter of GRNN to improve prediction performance. In order to verify and evaluate the performance of the proposed method, initial cycles data that have yet to exhibit apparent degradation is used. The comparison results show that RF-ABC-GRNN could reach lower test error than other methods even in earlier cycles. For example, the proposed method obtains a lower test error of 6.3% with the first 80 cycles than 9.1% in Ref. [24] (using the first 100 cycles). In summary, the proposed method RF-ABC-GRNN is a promising method in early-cycle stage RUL prediction.

Credit author statement

Zhang Yu: Conceptualization, Methodology, Software, Validation, Formal analysis, Investigation, Writing – original draft, Writing – review & editing, Visualization, Peng Zhen: Writing – original draft, Supervision, Guan Yong: Project administration, Supervision, Writing – review & editing. Wu Lifeng: Writing – review & editing, Supervision.

Declaration of competing interest

The authors declare that they have no known competing financial interests or personal relationships that could have appeared to influence the work reported in this paper.

Acknowledgement

This work was supported by the National Natural Science Foundation of China [grant numbers 61873175]; the Key Projects of Science and Technology Program of Beijing Municipal Education Commission (No.KZ202110017025, KZ201710028028); the Capacity Building for Sci-Tech Innovation—Fundamental Scientific Research Funds [grant number 025185305000-187]; the Youth Innovative Research Team of Capital Normal University; the academy for multidisciplinary studies of Capital Normal University; and the Beijing Youth Talent Support Program [grant number CIT&TCD201804036].

Appendix

Supplementary Table 1
Feature names and corresponding abbreviations.

	Features	Abbreviation
$\triangle Q_{100\text{-}10}(V)$ features	Minimum	Minimum of $\triangle Q_{100\text{-}10}(V)$
	Mean	Mean of $\triangle Q_{100\text{-}10}(V)$
	Variance	Variance of $\triangle Q_{100\text{-}10}(V)$
	Skewness	Skewness of $\triangle Q_{100\text{-}10}(V)$
	Kurtosis	Kurtosis of $\triangle Q_{100\text{-}10}(V)$
	Value at 2V	$\triangle Q_{100\text{-}10}$ (2)
Discharge capacity fade curve features	Slope of the linear fit to the capacity fade curve, cycles 2 to 100	$k_{2\text{-}100}$
	Intercept of the linear fit to capacity fade curve, cycles 2 to 100	$b_{2\text{-}100}$
	Slope of the linear fit to the capacity fade curve, cycles 91 to 100	$k_{91\text{-}100}$
	Intercept of the linear fit to capacity fade curve, cycles 91 to 100	$b_{91\text{-}100}$
	Discharge capacity, cycle 2	QD_2
	Difference between max discharge capacity and cycle 2	$QD_{M\text{-}2}$
	Discharge capacity, cycle 100	QD_{100}
Other features	Average charge time, first 5 cycles	$\overline{ct}_{1-5}$
	Maximum temperature, cycles 2 to 100	MAX $T_{2\text{-}100}$
	Minimum temperature, cycles 2 to 100	MIN $T_{2\text{-}100}$
	Integral of temperature over time, cycles 2 to 100	$\int T_{2-100}$
	Internal resistance, cycle 2	IR_2
	Minimum internal resistance, cycles 2 to 100	Min IR_2
	Internal resistance, difference	$IR_{100\text{-}2}$

References

[1] Xiong R, Tian J, Mu H, Wang C. A systematic model-based degradation behavior recognition and health monitoring method for lithium-ion batteries. Appl Energy 2017;207:372–83. https://doi.org/10.1016/j.apenergy.2017.05.124.

[2] Zhang X, Wang Y, Liu C, Chen Z. A novel approach of battery pack state of health estimation using artificial intelligence optimization algorithm. J Power Sources 2018;376:191–9. https://doi.org/10.1016/j.jpowsour.2017.11.068.

[3] Zheng Y, Gao W, Ouyang M, Lu L, Zhou L, Han X. State-of-charge inconsistency estimation of lithium-ion battery pack using mean-difference model and extended Kalman filter. J Power Sources 2018;383:50–8. https://doi.org/10.1016/j.jpowsour.2018.02.058.

[4] Meng J, Cai L, Stroe D-I, Ma J, Luo G, Teodorescu R. An optimized ensemble learning framework for lithium-ion Battery State of Health estimation in energy storage system. Energy 2020;206:118140. https://doi.org/10.1016/j.energy.2020.118140.

[5] Barré A, Deguilhem B, Grolleau S, Gérard M, Suard F, Riu D. A review on lithium-ion battery ageing mechanisms and estimations for automotive applications. J Power Sources 2013;241:680–9. https://doi.org/10.1016/j.jpowsour.2013.05.040.

[6] Fasahat M, Manthouri M. State of charge estimation of lithium-ion batteries using hybrid autoencoder and Long Short Term Memory neural networks. J Power Sources 2020;469:228375. https://doi.org/10.1016/j.jpowsour.2020.228375.

[7] Sun D, Yu X, Wang C, Zhang C, Huang R, Zhou Q, et al. State of charge estimation for lithium-ion battery based on an Intelligent Adaptive Extended Kalman Filter with improved noise estimator. Energy 2021;214:119025. https://doi.org/10.1016/j.energy.2020.119025.

[8] Khaleghi S, Firouz Y, Van Mierlo J, Van den Bossche P. Developing a real-time data-driven battery health diagnosis method, using time and frequency domain condition indicators. Appl Energy 2019;255:113813. https://doi.org/10.1016/j.apenergy.2019.113813.

[9] Li X, Yuan C, Wang Z. Multi-time-scale framework for prognostic health condition of lithium battery using modified Gaussian process regression and nonlinear regression. J Power Sources 2020;467:228358. https://doi.org/10.1016/j.jpowsour.2020.228358.

[10] Yang D, Zhang X, Pan R, Wang Y, Chen Z. A novel Gaussian process regression model for state-of-health estimation of lithium-ion battery using charging curve. J Power Sources 2018;384:387–95. https://doi.org/10.1016/j.jpowsour.2018.03.015.

[11] Shen D, Wu L, Kang G, Guan Y, Peng Z. A novel online method for predicting the remaining useful life of lithium-ion batteries considering random variable discharge current. Energy 2020:119490. https://doi.org/10.1016/j.energy.2020.119490.

[12] Qiu X, Wu W, Wang S. Remaining useful life prediction of lithium-ion battery based on improved cuckoo search particle filter and a novel state of charge estimation method. J Power Sources 2020;450:227700. https://doi.org/10.1016/j.jpowsour.2020.227700.

[13] Wang F-K, Mamo T. A hybrid model based on support vector regression and differential evolution for remaining useful lifetime prediction of lithium-ion batteries. J Power Sources 2018;401:49–54. https://doi.org/10.1016/j.jpowsour.2018.08.073.

[14] Li Y, Zou C, Berecibar M, Nanini-Maury E, Chan JC-W, van den Bossche P, et al. Random forest regression for online capacity estimation of lithium-ion batteries. Appl Energy 2018;232:197–210. https://doi.org/10.1016/j.apenergy.2018.09.182.

[15] Wu L, Fu X, Guan Y. Review of the remaining useful life prognostics of vehicle lithium-ion batteries using data-driven methodologies. Appl Sci 2016;6:166. https://doi.org/10.3390/app6060166.

[16] Chen L, Wang H, Liu B, Wang Y, Ding Y, Pan H. Battery state-of-health estimation based on a metabolic extreme learning machine combining degradation state model and error compensation. Energy 2021;215:119078. https://doi.org/10.1016/j.energy.2020.119078.

[17] Bian C, He H, Yang S. Stacked bidirectional long short-term memory networks for state-of-charge estimation of lithium-ion batteries. Energy 2020;191:116538. https://doi.org/10.1016/j.energy.2019.116538.

[18] Deng Z, Hu X, Lin X, Che Y, Xu L, Guo W. Data-driven state of charge estimation for lithium-ion battery packs based on Gaussian process regression. Energy 2020;205:118000. https://doi.org/10.1016/j.energy.2020.118000.

[19] Li X, Yuan C, Wang Z. State of health estimation for Li-ion battery via partial incremental capacity analysis based on support vector regression. Energy 2020;203:117852. https://doi.org/10.1016/j.energy.2020.117852.

[20] Wu J, Zhang C, Chen Z. An online method for lithium-ion battery remaining useful life estimation using importance sampling and neural networks. Appl Energy 2016;173:134–40. https://doi.org/10.1016/j.apenergy.2016.04.057.

[21] Chaoui H, Ibe-Ekeocha CC. State of charge and state of health estimation for lithium batteries using recurrent neural networks. IEEE Trans Veh Technol 2017;66:8773–83. https://doi.org/10.1109/TVT.2017.2715333.

[22] Yang F, Zhang S, Li W, Miao Q. State-of-charge estimation of lithium-ion batteries using LSTM and UKF. Energy 2020;201:117664. https://doi.org/10.1016/j.energy.2020.117664.

[23] Ma Y, Wu L, Guan Y, Peng Z. The capacity estimation and cycle life prediction of lithium-ion batteries using a new broad extreme learning machine approach. J Power Sources 2020;476:228581. https://doi.org/10.1016/j.jpowsour.2020.228581.

[24] Severson KA, Attia PM, Jin N, Perkins N, Jiang B, Yang Z, et al. Data-driven prediction of battery cycle life before capacity degradation. Nat Energy 2019;4:383–91. https://doi.org/10.1038/s41560-019-0356-8.

[25] Remeseiro B, Bolon-Canedo V. A review of feature selection methods in medical applications. Comput Biol Med 2019;112:103375. https://doi.org/10.1016/j.compbiomed.2019.103375.

[26] Breiman L. Random forests. Mach Learn 2001;45:5–32. https://doi.org/10.1023/A:1010933404324.

[27] Niu D, Wang K, Sun L, Wu J, Xu X. Short-term photovoltaic power generation forecasting based on random forest feature selection and CEEMD: a case study. Appl Soft Comput 2020;93:106389. https://doi.org/10.1016/j.asoc.2020.106389.

[28] Gregorutti B, Michel B, Saint-Pierre P. Correlation and variable importance in random forests. Stat Comput 2017;27:659–78. https://doi.org/10.1007/s11222-016-9646-1.

[29] Specht DF. A general regression neural network. IEEE Trans Neural Network 1991;2:568–76. https://doi.org/10.1109/72.97934.

[30] Liang Y, Niu D, Hong W-C. Short term load forecasting based on feature extraction and improved general regression neural network model. Energy 2019;166:653–63. https://doi.org/10.1016/j.energy.2018.10.119.

[31] Antanasijević D, Pocajt V, Ristić M, Perić-Grujić A. Modeling of energy consumption and related GHG (greenhouse gas) intensity and emissions in Europe using general regression neural networks. Energy 2015;84:816–24. https://doi.org/10.1016/j.energy.2015.03.060.

[32] Karaboga D, Akay B. A comparative study of Artificial Bee Colony algorithm. Appl Math Comput 2009;214:108–32. https://doi.org/10.1016/j.amc.2009.03.090.

[33] Patil MA, Tagade P, Hariharan KS, Kolake SM, Song T, Yeo T, et al. A novel multistage Support Vector Machine based approach for Li ion battery remaining useful life estimation. Appl Energy 2015;159:285–97. https://doi.org/10.1016/j.apenergy.2015.08.119.

[34] Zhou J, He Z, Gao M, Liu Y. Battery state of health estimation using the generalized regression neural network. In: 2015 8th Int. Congr. Image signal process.; 2015. p. 1396–400. https://doi.org/10.1109/CISP.2015.7408101.

[35] Wang Y, Ni Y, Lu S, Wang J, Zhang X. Remaining useful life prediction of lithium-ion batteries using support vector regression optimized by artificial bee Colony. IEEE Trans Veh Technol 2019;68:9543–53. https://doi.org/10.1109/TVT.2019.2932605.

[36] Bendu H, Deepak BBVL, Murugan S. Multi-objective optimization of ethanol fuelled HCCI engine performance using hybrid GRNN–PSO. Appl Energy 2017;187:601–11. https://doi.org/10.1016/j.apenergy.2016.11.072.